

Russian Academy of Sciences
Joint Institute for High Temperatures RAS
Institute of Problems of Chemical Physics RAS
Kabardino-Balkarian State University

Physics of Extreme States of Matter — 2012

Chernogolovka, 2012

Physics of Extreme States of Matter — 2012

Edited by academician Fortov V. E., Karamurzov B. S., Efremov V. P., Khishchenko K. V., Sultanov V. G., Levashov P. R., Andreev N. E., Kanel G. I., Iosilevskiy I. L., Milyavskiy V. V., Mintsev V. B., Petrov O. F., Savintsev A. P., Shpatakovskaya G. V.

This compendium is devoted to investigations in the fields of thermal physics of extreme states of matter and physics of high energy densities. Different models and results of theoretical calculations of equations of state for materials at high pressures and temperatures, physics of shock and detonation waves, experimental methods of diagnostics of ultrafast processes, techniques of intense energy fluxes generation, interaction of intense laser, x-ray and microwave radiation, powerful particle beams with matter, low-temperature plasma physics, issues of physics and power engineering, as well as technology projects are considered. The majority of the works has been presented at the XXVII International Conference on Equations of State for Matter (March 1–6, 2012, Elbrus, Kabardino-Balkaria, Russia). The edition is intended for specialists in physical and technical problems of power engineering.

The conference is sponsored by the Russian Academy of Sciences and the Russian Foundation for Basic Research (grant No. 12-02-06011).

The editorial board announces with deep regret the death of the colleague and friend, Prof. Anatoliy Inderbievich Temrokov (January 17, 1942–February 22, 2011), who was the initiator, organizer, and chairman of the I All-Union Conference on Equations of State for Matter (together with Prof. D. A. Kirzhnits), the unchallenged chairman of 25 subsequent Conferences on Equations of State for Matter and Interaction of Intense Energy Fluxes with Matter.

CONTENTS

CHAPTER 1. EQUATIONS OF STATE FOR MATTER

<i>Shpatakovskaya G.V.</i> Semiclassical method in problems of quantum physics	6
<i>Chentsov A.V., Levashov P.R.</i> <i>Ab initio</i> calculation of compression isentrope of deuterium	9
<i>Knyazev D.V., Levashov P.R.</i> <i>Ab initio</i> calculation of static and dynamic conductivity of aluminum	12
<i>Dyachkov S.A., Levashov P.R.</i> Region of validity of Thomas–Fermi model and its thermal part	14
<i>Volkov N.B., Chingina E.A., Boltachev G.Sh.</i> Wideband two-temperature equation of state for metals at high energy densities	17
<i>Borovikov D.S., Iosilevskiy I.L.</i> Semi-analytical calculations for parameters of boiling layer in isentropic expansion of warm dense matter with van der Waals equation of state	19
<i>Zilevich A., Iosilevskiy I.L., Chigvintsev A.Yu.</i> Boundaries of thermodynamic stability for wide-range analytic EOS of fully ionized electron-ionic plasmas	23
<i>Bel'kheeva R.K.</i> Thermodynamic equation of state used to describe the behavior of a porous mixture	25
<i>Chigvintsev A.Yu., Iosilevskiy I.L.</i> Anomalous scenario for spinodal decomposition of metastable melting in the zero-temperature limit	28
<i>Soloviev A.M., Iosilevskiy I.L., Gryaznov V.K.</i> Properties of high-temperature phase diagram and critical point parameters in silica	31
<i>Rusin S.P.</i> On methods and criterions of true temperature determination of opaque heated bodies via thermal radiation spectrum	34
<i>Fortova S.V.</i> Spectrum analysis of the vortex cascades in homogeneous turbulent flow	36

CHAPTER 2. SHOCK WAVES. DETONATION. COMBUSTION

<i>Khokhlov V.A., Inogamov N.A., Zhakhovsky V.V., Anisimov S.I., Petrov Yu.V.</i> The structure of superelastic&plastic shock wave	39
<i>Mayer A.E., Khishchenko K.V., Levashov P.R., Mayer P.N.</i> High-rate dislocation plasticity and shock waves attenuation in metals	41
<i>Nikolayev A.Yu., Vildanov V.G., Borshchevsky A.O., Tkachyov O.V., Zaikin V.T., Slobodenyukov V.M.</i> Sound velocity in shock-compressed polytetrafluoroethylene in stress range 1.5–45 GPa	44
<i>Bordzilovskii S.A., Karakhanov S.M., Khishchenko K.V.</i> Brightness temperature and physical-chemical transformation of the epoxy system EC141NF under shock-wave loading conditions	46
<i>Efremov V.P., Frolov A.A., Dianov E.M., Bufetov L.A., Fortov V.E.</i> Experimental investigation of laser supported detonation	49
<i>Yankovskiy B.D., Milyavskiy V.V.</i> Study of RDX detonation at non-ideal regimes	51
<i>Konyukhov A.V., Likhachev A.P.</i> Influence of packing fraction in a hard-sphere EOS on focusing of cylindrical shock waves	54
<i>Gvozdeva L.G., Gavrenkov S.A.</i> Analytical determination of boundaries of existence of triple shock wave configuration with a negative angle of reflection in steady supersonic flow	57
<i>Gavrenkov S.A., Gvozdeva L.G.</i> A new type of triple configuration in steady supersonic flow	59
<i>Khramtsov P.P., Penyazkov O.G., Shatan I.N., Chernik M.Yu.</i> The application of the Talbot effect for the measurements of dispersion characteristic of refractive index in axisymmetric methane jet flame	61
<i>Krivokorytov M.S., Golub V.V.</i> Acoustic influence on methane diffusion flame	63
<i>Leschevich V.V., Penyazkov O.G., Evmenchikov N.L.</i> Auto-ignition of hydrogen-air mixtures at intermediate temperatures in rapid compression machine	64
<i>Golovastov S.V., Golub V.V.</i> Ignition delays for diffusion self-ignition of hydrogen discharged under high pressure into air	67
<i>Bocharnikov V.M., Mikushkin A.Yu., Golovastov S.V.</i> On characteristics of hydrogen self-ignition at pulse discharge into channel	70
<i>Mikushkin A.Yu., Golovastov S.V., Baklanov D.I.</i> Specific impulse of nozzle of the pulse engine	72
<i>Bivol G.Y., Lenkevich D.A., Mirova O.A., Danilov A.P., Kotelnikov A.L., Bazhenova T.V.</i> Shock wave reflection from obstacle made of easily destructible granular material	74
<i>Doroshko M.V., Penyazkov O.G.</i> High temperature decay of hydrocarbons behind the reflected shock waves and dynamics of soot formation	77

CHAPTER 3. POWER INTERACTION WITH MATTER

<i>Povarnitsyn M.E., Andreev N.E., Levashov P.R., Khishchenko K.V., Rosmej O.N.</i> Application of thin metal foils for contrast improvement in experiments with intensive high-energy laser pulses	80
<i>Abrosimov S.A., Bazhulin A.P., Voronov V.V., Krasnyuk I.K., Pashinin P.P., Semenov A.Yu., Stuchebryukhov I.A., Khishchenko K.V.</i> Study of matter properties at negative pressures using picosecond laser pulses	85

<i>Petrov Yu.V., Inogamov N.A.</i> Thermal conductivity due to s-s and s-d electron interaction in nickel at high electron temperatures	87
<i>Agranat M.B., Andreev N.E., Chefonov O.V., Ovchinnikov A.V., Rosmej O.N., Petrovskiy V.P.</i> Experimental investigation of a quantum yield of a characteristic x-ray radiation at interaction of femtosecond s-polarized laser pulses with nanostructured Cu targets	90
<i>Kostenko O.F., Andreev N.E.</i> On the characteristic x-ray yield from the targets irradiated by femtosecond laser pulses	92
<i>Kasparov K.N., Ivlev G.D., Belaziorava L.I., Gatskevich E.I.</i> Fast response time temperature measurements at pulsed laser irradiation of different materials	95
<i>Andreev N.E., Baranov V.E.</i> PIC simulation of the laser wakefield acceleration: LAPLAC and WAKE-EXI codes comparison	97
<i>Khokonov M.Kh.</i> Strong field multi photon effects in interaction of high energy electrons with oriented crystals	99
<i>Yanilkin I.V., Velichko A.M., Shkol'nikov E.I.</i> Investigation of AlO molecules emission formation obtained by Al target vaporization by radiation of pulsed CO ₂ -laser	102
<i>Savintsev A.P., Gavasheli Yu.O.</i> Study of breakdown mechanism of optically transparent dielectrics by focused laser beam	104
<i>Veleschuk V.P., Vlasenko A.I., Gatskevich E.I., Gnatyuk V.A., Ivlev G.D., Levytskyi S.N., Aoki T.</i> Laser doping of CdTe by In	105
<i>Dvoretzky S.A., Gatskevich E.I., Ivlev G.D., Mikhailov N.N., Shimko A.N.</i> Nanopulsed laser action on Cd _x Hg _{1-x} Te layers	108
<i>Yanilkin A.V.</i> Recombination of point defects in Mo under irradiation. Molecular dynamics simulation	110
<i>Mayer P.N., Khishchenko K.V., Levashov P.R., Mayer A.E.</i> Kinetics of metal evaporation and condensation under the high-current electron irradiation	113
<i>Pronkin A.A., Kostanovskiy A.V.</i> Conditions of formation carbyne thin films by magnetron sputtering of graphite target	116

CHAPTER 4. PHYSICS OF LOW TEMPERATURE PLASMA

<i>Pinchuk M.E., Bogomaz A.A., Budin A.V., Rutberg Ph.G., Losev S.Yu., Pozubenkov A.A., Svetova V.Yu.</i> Z-pinch in helium at initial pressure of 10–25 MPa	118
<i>Volkov N.B., Barakhvostov S.V., Nagayev K.A., Bochkarev M.B., Tarakanov V.P., Tkachenko S.I., Chingina E.A.</i> Plasma channel structure during the high-voltage generator with the picosecond pulse front discharge to the microwires	120
<i>Tkachenko S.I., Zhakhovsky V.V., Shelkovenko T.A., Pikuz S.A.</i> Phase evolution of dense core during aluminum wire explosion	123
<i>Yankovskiy B.D.</i> Dense plasma in high current systems with large density of energy	125
<i>Filinov V.S., Bonitz M., Fehske H., Fortov V.E., Levashov P.R.</i> Phase diagram of strongly coupled dense hydrogen by path-integral Monte Carlo	128
<i>Filinov V.S., Bonitz M., Ivanov Yu.B., Levashov P.R., Fortov V.E.</i> Thermodynamics of strongly coupled quark-gluon plasma by path integral Monte Carlo method in grand canonical ensemble	131
<i>Zaporozhets Yu.B., Mintsev V.B., Gryaznov V.K., Fortov V.E., Winkel M., Reinholz H., Röpke G.</i> Laser radiation interaction with strongly correlated plasma	133
<i>Kazeev N.A., Morozov I.V., Valuev I.A.</i> Wave packet molecular dynamics with packet splitting	136
<i>Bystryi R.G., Morozov I.V.</i> GPU-accelerated molecular dynamics simulations of nonideal plasmas	139
<i>Ivanovskis G., Norman G.E., Stegailov V.V., Usmanova D.R.</i> Anomalous diffusivity of ionic liquids. Classical molecular dynamics study	141
<i>Usmanova D.R., Ivanovskis G., Norman G.E.</i> Stochastic properties of ionic liquid	144
<i>Savin S.F., D'yachkov L.G., Myasnikov M.I., Petrov O.F., Vasiliev M.M., Fortov V.E., Kaleri A.Yu., Borisenko A.I.</i> Coulomb ensemble of charged diamagnetic macroparticles in a magnetic trap under microgravity conditions	146
<i>Lapitsky D.S.</i> Dynamic dust particle confinement in gas flow	149
<i>Antipov S.N., Vasiliev M.M., Petrov O.F.</i> The possibilities of cryogenic temperatures for dusty plasma structure formation	151
<i>Zolnikov K.P., Abdrashitov A.V., Psakhie S.G.</i> Behavior of bicomponent dusty plasma clusters under electric pulsed loading	154
<i>Dudin S.V., Kozlov A.V., Leontev A.A., Mintsev V.B., Fortov V.E., Shurupov A.V., Shurupova N.P., Zavalova V.E., Ushnurtsev A.E.</i> Two-stage explosive magnetic generator with disconnecting of the primary circuit current	155
<i>Kurilenkov Yu.K., Karpukhin V.T., Gus'kov S.Yu.</i> On DD synthesis at inertial electrostatic confinement scheme based on low energy vacuum discharge with deuterium-loaded Pd anode	157
<i>Glushniova A.V., Saveliev A.S.</i> Experimental study of gas outflow from discharge chambers	160

<i>Klementyeva I.B., Moralev I.A.</i> Electrical discharge influence on parameters and structure of gas flows in external magnetic field	162
<i>Kuznetsov D.L., Filatov I.E., Surkov Yu.S., Uvarin V.V., Ugodnikov G.G., Nikiforov S.A.</i> Installation for research of CS ₂ conversion processes in streamer corona generated plasma	164
<i>Kiselev V.I., Polistchok V.P., Samoylov I.S.</i> Arc discharge between graphite electrodes at low pressure of argon	167
<i>Daryan L.A., Kozlov A.V., Kotov A.V., Povareshekin M.N., Polistchok V.P., Shurupov A.V., Shurupova N.P.</i> Pulse arc discharge in mineral and organic oils	168

AUTHOR INDEX	170
-------------------------------	-----

ABBREVIATIONS	172
--------------------------------	-----

THE STRUCTURE OF SUPERELASTIC&PLASTIC SHOCK WAVE

*Khokhlov V.A.,^{*1} Inogamov N.A.,¹ Zhakhovsky V.V.,² Anisimov S.I.,¹ Petrov Yu.V.¹*

¹*ITP RAS, Chernogolovka, ²JIHT RAS, Moscow, Russia, USF, Tampa, United States*

^{*}*v_a_kh@mail.ru*

Last year we have reported the observation of superelastic shock waves [1, 2]. These waves move with the “elastic” velocity (in a continual approach this velocity is defined by the elastic constant $K + \frac{4}{3}G$ contrary to the velocity of plastic wave, which is defined by the elastic constant K). Here K and G are bulk and shear moduli of a material. However, the pressure behind the shock wave is several times the classical Hugoniot elastic limit. Such waves have been observed in experiments for example [3–7]. The motion of a shock wave and the subsequent plastic shock are correlated. Now we present the structure of superelastic&plastic shock wave on the base of molecular-dynamic simulation [2, 8]. The calculations correspond conditions of the experiment [3]: a laser pulse with duration of 120 fs and a power of $7.7 \cdot 10^{13}$ W/cm² (the absorbed energy is 2.6 J/cm²) affects the aluminum film.

The initial elastic shock wave (ELSW) begins to form well before the maximum of compression wave on the front of melting (see Fig. 1, 2).

The thermal wave leaves far forward at a two-temperature stage due to the fact that the thermal diffusivity of the electron subsystem $\chi_e = \kappa_e/c_e$ is much more than the one of a whole substance $\chi = \kappa_e/c$ (here c_e and c are the heat capacities of electron subsystem and whole matter respectively, and the heat con-

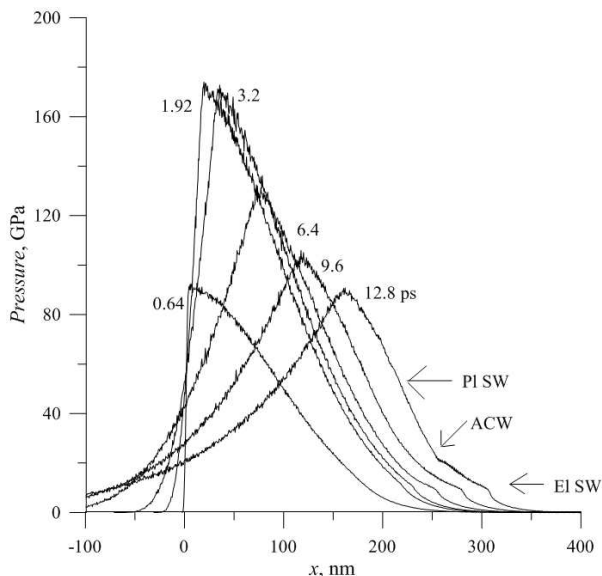


Figure 1. Pressure profiles at short time. The numbers on the curves specify time in ps. The arrows indicate the sites with the greatest steepness of the pressure profile of which elastic (ELSW) and the plastic wave (PISW) shock waves are further formed, and the break of the pressure profile at the boundary of the elastic and plastic zones from which additional compression wave radiates (ACW)

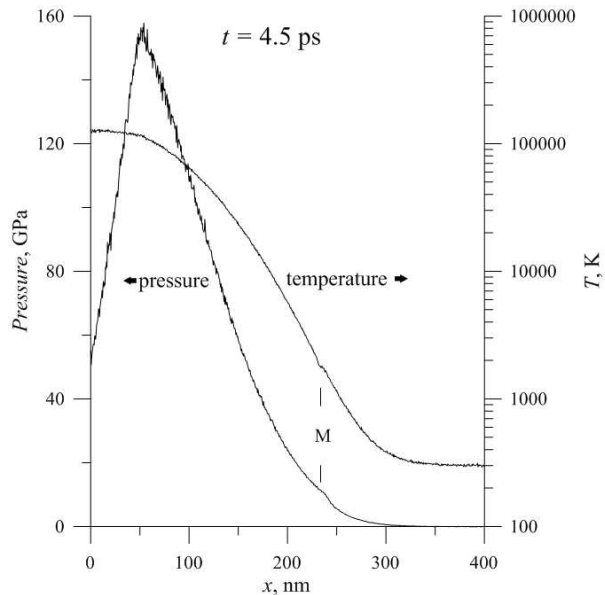


Figure 2. Pressure p_{xx} and temperature at $t = 6.4$ ps. Lines M indicated position of melting front

ductivity of a matter is determined dominantly by the electron heat conductivity κ_e). When passing through the melting front the pressure profile becomes steeper. This creates the seed from which the leading elastic shock wave develops (Fig. 2).

The pressure on the elastic shock wave at this time is close to the Hugoniot elastic limit (HEL, for aluminum the part of GPa). Then the elastic shock quickly passes the front of melting.

Emerging plastic shock (PISW) overtakes and pushes the emerging elastic one. The pressure in the metastable elastically compressed material behind the elastic shock rises to a value several times larger than HEL (in aluminum up to tens of GPa). Ahead of the PISW there arise additional compression waves (ACW) (see Fig 3, 4). The fact that the material remains elastically deformed after the first front and experiences plastic deformations on the second front can be seen from the profiles of shear stress (dashed lines in Fig. 3 and following figures), which is proportional to the pressure at uniaxial shear in an elastic material and is reset to zero by plastic deformations. The pressure on ACW is higher than on the ELSW. They move also in an elastic medium. Following one after another, these waves are catching up ELSW and push it (see Fig. 5).

In the advanced stage long time elastic shock moves with its “elastic” rate (taking into account the contribution of shear stresses under uniaxial compression) and plastic shock moves together with it almost simultaneously. Then the plastic wave gradually loses its

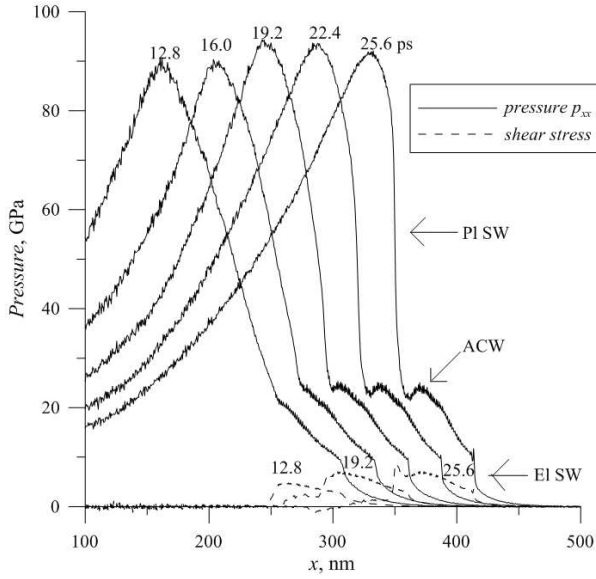


Figure 3. Formation of elastic (EISW) and plastic (PISW) shock waves and additional compression (ACW) wave between them. Pressure profiles (continuous lines) and shear stress (shaped lines) are shown. The numbers on the curves specify time in ps.

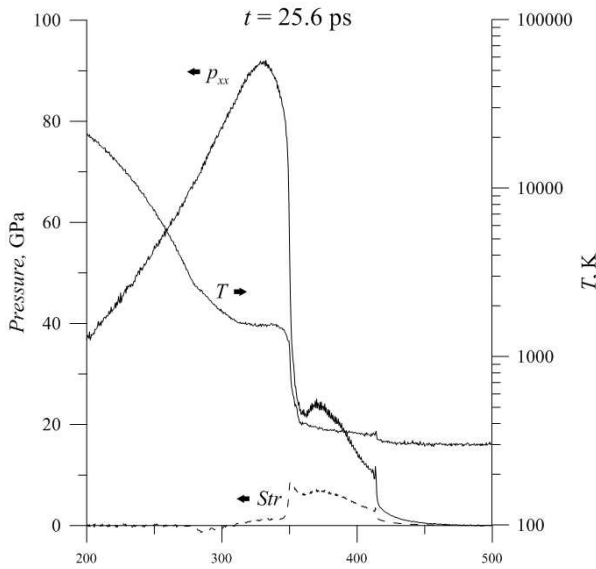


Figure 4. Pressure p_{xx} and shear stress and temperature at $t = 25.6$ ps

intensity and slowed down (see Fig. 6). Finally the plastic wave stops. Plastically deformed layer of a final thickness is thus fixed.

The resulting graphics of a motion of elastic and plastic shock waves and additional compression waves in comparison with the shock wave in two-temperature hydrodynamic calculations (2T-HD) without taking into account the elastic corrections are shown in Fig. 7. With the coexistence of several compression waves there are plotted the coordinates of stronger one. We can see the jumps in the graph of compression waves in passing from one wave to another. At large times when the plastic shock wave decays it is shown the position of the front of plastic deformations.

The simulation results well correspond to results of

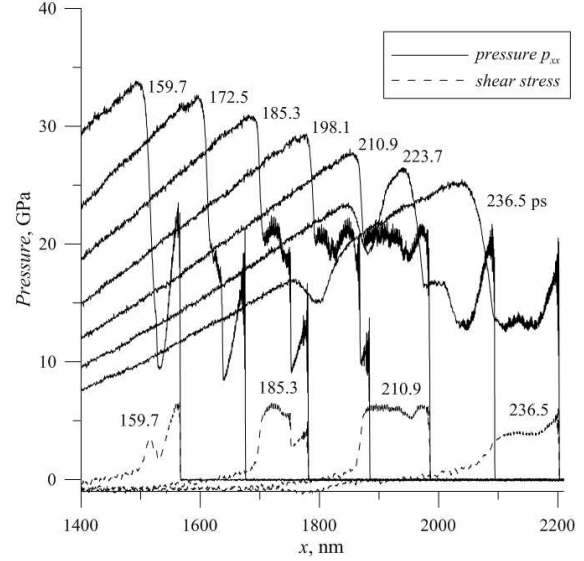
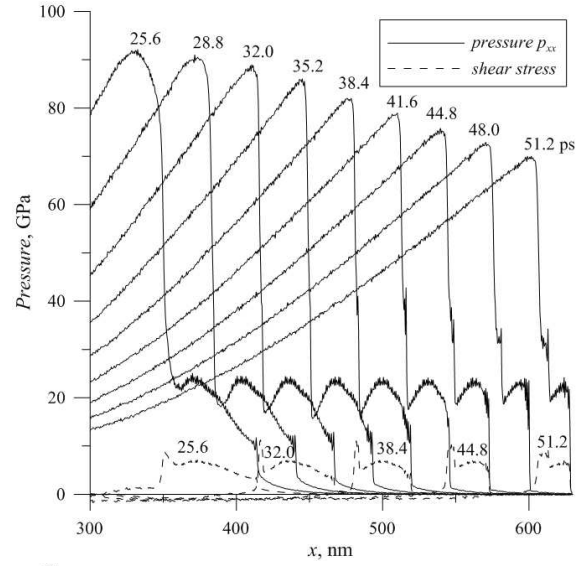


Figure 5. Superelastic&plastic wave structure at medium times.

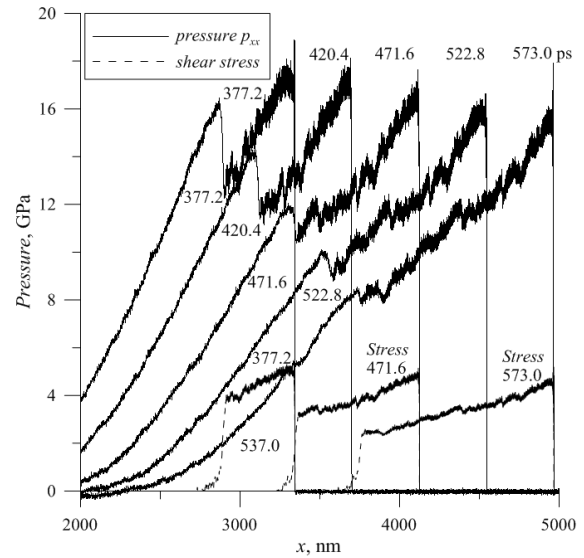


Figure 6. Attenuation and braking of a plastic wave on large times. Pressure profiles (continuous lines) and shear stress (shaped lines) are shown. The numbers on the curves specify time in ps.

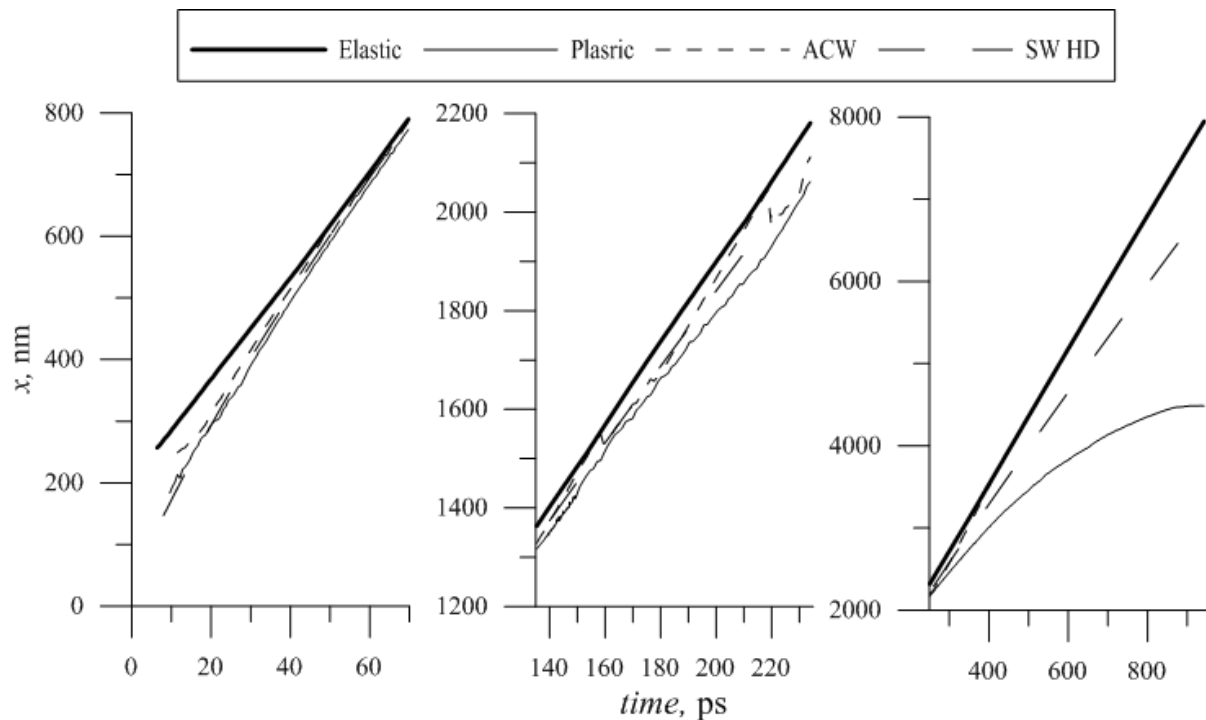


Figure 7. The elastic SW (thick lines), the plastic wave / plastic deformations front (thin lines), additional compression waves (short dashed lines) and SW position from 2T-HD calculations (long dashed lines)

experiments [3] (see [2, 8]). At large times the position of ELSW corresponds to the results of experiments [4], which have been performed with the same characteristics of the laser pulse as [3], but with thicker films.

This work was supported by the RAS program “Thermophysics and mechanics of extreme energy action and physics of highly compressed matter” and RFBR grant 10-02-00434-a.

1. Inogamov N. A., Khokhlov V. A., Zhakhovskii V. V. // *Physics of Extreme States of Matter—2011* / Ed. by Fortov V. E., et al. Chernogolovka: IPCP RAS, 2011. P. 11–14.
2. Inogamov N. A., Zhakhovskii V. V., Khokhlov V. A., Shepelev V. V. // *JETP Lett.* 2011. V. **93**. P. 226–232
3. Evans R., Badger A. D., Fallies F., Mahdiah M., and Hall T. A. // *Phys. Rev. Lett.* 1996. V. **77**. P. 3359.
4. Huang Li, Yang Y., Wang Y., Zheng Z. and Su W. //

- J. Phys. D: Appl. Phys. 2029. V. **42**. P. 045502.
5. Agranat M. B., Anisimov S. I., Ashitkov S. I., Zhakhovskii V. V., Inogamov N. I., Komarov P. S., Ovchinnikov A. V., Fortov V. E., Khokhlov V. A., Shepelev V. V. // *JETP Letters.* 2010. V. **91**. P. 471 [Pis'ma v ZhETF. 2010. V. **91**. No. 9 P. 517–523]
6. Ashitkov S. I., Agranat M. B., Kanel' G. I., Komarov P. S. and Fortov V. E. // *JETP Letters.* 2010. V. **92**. No. 8. P. 516 [Pis'ma v ZhETF. 2010. V. **92** No. 8. P. 568–573]
7. Whitley V. H., McGrane S. D., Eakins D. E., Bolme C. A., Moore D. S., and Bingert J. F. // *J. Appl. Phys.* 2011. V. **109**. P. 013505
8. Inogamov N. A., Khokhlov V. A., Petrov Yu. V., Anisimov S. I., Zhakhovskii V. V., Demaske B. J., Oleynik I. I., White C. T., Ashitkov S. I., Khishchenko K. V., Agranat M. B. and Fortov V. E. // *AIP Conference Proceedings.* 2012. V. **1426**, in press.

HIGH-RATE DISLOCATION PLASTICITY AND SHOCK WAVES ATTENUATION IN METALS

*Mayer A.E.,^{*1} Khishchenko K.V.,² Levashov P.R.,² Mayer P.N.¹*

¹CSU, Chelyabinsk, ²JiHT RAS, Moscow, MIPT, Dolgoprudny, Russia

*mayer@csu.ru

Introduction. In the present work, we develop the theoretical approach for high-rate dislocation plasticity proposed in [1–3]. Plastic strain rate is found out through the dislocations sliding; equations for kinetics and motion of dislocations contain pseudo-relativistic terms.

In papers [1–3] a good agreement had been obtained with experimental data for elastic precursor shape and height for a number of metals (copper, aluminum, iron,

titanium); but an agreement for the unloading wave shape was not so good. It should be note that similar problem with the unloading wave modeling was met by other researches as well [4]. Possible reason of such deviation is a formation of various dislocation structures, as it was pointed out in [3].

As opposed to [1–3], more complex kinetic equations are used here, which take into account the mobile dislocations and another type of dislocations, which